Asian Journal of Chemistry; Vol. 31, No. 8 (2019), 1871-1876

ASIAN JOURNAL OF CHEMISTRY

https://doi.org/10.14233/ajchem.2019.22039

Molecular Structure and Spectral Characterization of Diamagnetic Co(III) Complex Incorporating Hexaadentate Schiff Base Ligand

EIDA S. AL-FARRAJ[1], AMANI S. ALTURIQI[2], MUREFAH M. ANAZY[2] and RE[illegible] AMM[illegible]

[1]Department of Chemistry, College of Science, Imam Mohammad Ibn Saud Islamic University[illegible]623 Ri[illegible]Saudi A[illegible]ra
[2]Department of Chemistry, College of Science, Princess Nourah bint Abdul Rahman Unive[illegible], Riyadh, Saud[illegible]

*Corresponding author: E-mail: dr_redaammar@yahoo.com

Received: 27 February 2019; *Accepted*: 20 May 2019; *Published online*: 28 [illegible]019; AJC-19468

A novel Co(III) complex derived from hexaadentate Schiff base ligand, H[illegible] was describe[illegible]e ligand is prepared from the reaction of *tris*-2-aminoethyl amine and *o*-vanillin in 1:3 molar ratio. The structure [illegible] ligand and i[illegible]o(III) complex was described by micro-analyses, FT-IR, NMR, ESI-MS and UV/visible and thermal stability. DF[illegible] was car[illegible]out to get insights into the ligand and its Co(III) complex to compare the values of bond lengths and angles with ea[illegible]electronic spectra, Mulliken atomic charge distribution, HOMO-LUMO energy and the thermodynamic [illegible]ters have been calculated.

Keywords: Co(III) complex, DFT studies, Schiff base liga[illegible]Structu[illegible]terization.

INTRODUCTION

The chemistry of Schiff bases have [illegible]acted v[illegible]dwide attention because of their flexible nature a[illegible]e i[illegible] from one pot condensation of prim[illegible] alip[illegible]r aromatic amines and carbonyl compound[illegible]2]. Moreo[illegible]e Schiff bases as coordinating ligands [illegible]xtensive appli[illegible]ns in chemistry and biochemistry [illegible]po[illegible]significant biological activity [3-6]. Recently, there is rapid g[illegible]h in coordination chemistry of Schiff base[illegible]nds [7-9]. *Tris*([illegible]oethyl)amine, a commercially avail[illegible]tripodal amine, has sh[illegible]wn tremendous applications as a l[illegible]d [10][illegible]ver the years, the hexadentate H_3L, obtained t[illegible]con[illegible]sation r[illegible]ction of *tris*-2-amino-ethyl-amine and sa[illegible]ehyde o[illegible]close analogues have been studi[illegible]xtensiv[illegible]e to[illegible]r flexible nature around aminoe[illegible]s in co[illegible]on with the rigidity of the salic[illegible]ene un[illegible]o make eas[illegible] in the encapsulation of metal io[illegible]1-19].

[illegible]rk, we described the synthesis of H_3L derived from *tri*[illegible]ainoethyl-amine and *o*-vaniline and its Co(III) complex fol[illegible]by the investigations of their neuromodulatory properties. DF[illegible]d DFT (TD-DFT) calculations are achieved to obtain insights into the structure of H_3L and its Co(III) complex to gain information of better understanding of the [illegible]eometrical and electronic properties and to show the des-[illegible]ption of the spectroscopic assignments of the UV-visible including HOMO, LUMO, MEP and Mulliken atomic charge distribution.

EXPERIMENTAL

The elemental analyses (CHN) of synthesized H_3L and its Co(III) complex were recorded using ElementarVarrio EL analyzer. The electronic spectra were collected using LKB-Biochem, UV-visible spectrophotometer at room temperature in ethanol. FT-IR spectra of H_3L and its Co(III) complex were obtained as a KBr pellet using Perkin Elmer 621 spectrophotometer at 4000-400 cm^{-1}. SDTQ-600 (TA) was used to study the thermal behaviour of the complex in helium (100 mL min^{-1}). The ESI-MS spectra of H_3L and its Co(III) complex were determined using Agilent technologies Ion trap LC/MS 6320.

Synthesis of ligand, H_3L: *Tris*(2-aminoethyl)amine (100 mg, 0.684 mol) was added into the alcoholic solution of *o*-vanillin (311 mg, 2.05 mol) at room temperature in 1:3 molar ratio followed by vigorous stirring for 10 h. The filtrate was collected and yellow microcrystalline product was obtained upon evaporation at room temperature.

Yield: 87 %, Anal. of H_3L calcd. for $C_{30}H_{36}N_4O_6$: C, 65.68; H, 6.61; N, 10.21. F.: C, 65.61; H, 6.56; N, 10.15 %; ESI-MS

m/z: 550.25, ^{1}H NMR (400 MHz, $(CH_3)_2SO$-d_6, ppm): 8.22 (s, C **H**=N, 3H), 6.56-6.94 (m, 9H, **H**-Ar), 3.71 (s, 9H, -OC**H**$_3$), 1.93 (-C**H**$_2$-), 1.89 (-C**H**$_2$-): ^{13}C NMR (DMSO-d_6, ppm): 166.9 (-**C**H=N), 153.2 (-**C**-OH), 148.7 (-**C**-O-CH$_3$), 123.7-115.0 (Ar-**C**), 56.6 (-CH$_2$-**C**H$_2$-), 56.2 (-CH$_2$-**C**H$_2$-), 55.4 (-O-**C**H$_3$); IR (KBr pellet, cm^{-1}): 1645 ν(CH=N),

Synthesis of Co(III) complex: To an alcoholic solution of ligand, H_3L (100 mg, 0.182 mol) mixed with catalytic amount of trimethylamine was added hydrated Co(III) chloride was stirred for 10 h, which led to the formation of slight white turbidity. Yellow coloured microcrystalline product was obtained in few days.

Yield: 72 %; Anal. calcd. for $C_{30}H_{33}N_4O_6Co$: C, 58.97; H, 5.44; N, 9.17. Found: C, 58.89; H, 5.38; N, 9.12 %; ESI-MS *m/z*: 610.17, ^{1}H NMR (400 MHz, $(CH_3)_2SO$-d_6, ppm): 8.21 (s, 3H, -C**H**=N), 6.56-7.10 (m, 9H, Ar-**H**), 3.85 (s, 9H, -O-C**H**$_3$); 2.87 (-C**H**$_2$), - 2.79 (-C**H**$_2$); ^{13}C NMR: 170.5 (-**C**H=N), 157.5 (-**C**-O-), 135.5-120.4 (Ar-**C**); IR (KBr pellet, cm^{-1}): 1625 ν(CH=N).

Computational procedures: All quantum chemical computations of H_3L and its Co(III) complex were achieved by using G16W suit of programs [20]. The optimized molecular studies of H_3L and its Co(III) complex were measured in the gas phase at DFT B3LYP/6-31 + G(d,p) level of theory. Fukui functions of H_3L and its Co(III) complex were calculated by using DMol3 [21,22] and B3LYP/DND programs [23].

RESULTS AND DISCUSSION

The analytical data characterization is quite close to proposed structure of ligand and its Co(III) complex. The synthesized H_3L upon complexation with $CoCl_2$ in 1:1 molar ratio yields Co(III) complex (**Scheme-I**). Presence of strong stretching vibration due to azomethine group at 1640 cm^{-1} in the synthesized H_3L indicates that the NH_2 group condensed [24,25]. Furthermore, the IR spectrum demonstrates band at 3000-2150 cm^{-1} which assigned inter-moleclar hydrogen bonding interaction between the NH nitrogen and the α-C_6H_5-OH proton [26]. Interestingly, the azomethine band is dropped upon complexation and observed at 1625 cm^{-1} [27]. Furthermore, the IR spectrum of H_3L shows the aromatic vibrations due to C=C bond and C-H bond at 1575-1520 and 756-750 cm^{-1}, respectively [28]. However, these positions shifted upon complexation. The presence of a broad band at 3215-3225 cm^{-1} in the Co(III) complex suggests the presence of water [29].

The ^{1}H NMR spectra of H_3L exhibit a singlet at 8.22 ppm assigned to CH=N resonance, which gets strong support due to the existence of sharp signal at 166.9 ppm assigned to azomethine carbon in ^{13}C NMR. The proton resonance due to NH group appeared at 3.71 ppm. However, the signal due to CH_3 group in ^{13}C NMR appeared at 56.2 ppm. Furthermore, proton resonance due to -CH_2/-CH_2 protons were observed at 1.89-193 ppm in the free ligand where the signal due to CH_2 and aromatic carbons appeared at 56.2-115.0-153.2 ppm, respectively in the ligand. The resonances due to various hydrogen atoms are consistent to the structure of Co(III) complex and show a multiplets at 6.57-7.10 ppm attributed to aromatic protons of vanillin moiety in the complex. The signals due to methoxyl protons of methoxy group appeared as singlet at 3.85 ppm and the signals due to methylene protons appeared at 1.89-2.87 ppm. However, the signals in ^{13}C NMR signals show deshielding upon complexation of ligand to cobalt(III) ion.

To check the thermal stability of the complex, thermal study recorded which showed degradation of complex in three steps. First degradation step occurred at 130-150 °C, indicated to the loss of moisture and assigned is to 5.56 %. The second degradation step is the main decomposition step and occurred at 400-500 °C and leads to the 48 % which is equivalent to the loss of the two salen moietes. However, the remaining organic moiety which is equivalent to 35.33 % is decomposed at temperature 750 °C in third and final step, leaving behind Co_2O_3 corresponding to 12.67 % of the total weight of complex.

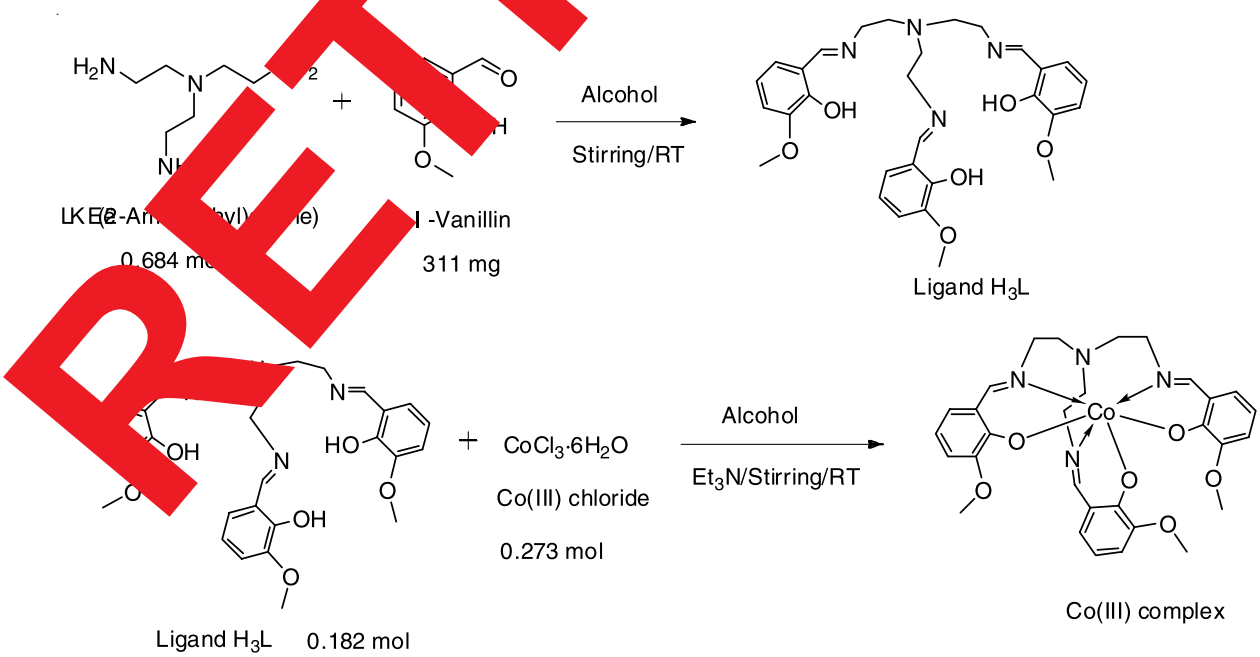

Scheme-I: Synthetic method of H_3L and its Co(III) complex

Molecular geometry: Ligand H_3L and Co(III) complex is fully optimized in gas phase applying DFTB3LYP/6311TD (d,p) basis set in term of energy. Fig. 1 shows the numbering of the complex atoms used to calculate the bond distances and bonds angle of H_3L and complex. H_3L (Fig. 1a) of complex coordinates through azomethine and deprotonated hydroxyl oxygen to Co(III) ion. The optimized Co(III) complex (Fig. 1b) indicates the distorted geometry of the structure around the center of the metal. The bond distances calculated around the center of cobalt is slightly longer compared to free ligand. Elongation in bond lengths might be possible because of the electron shifting from ligand to metal. The ligand with a planar structure loses its planarity after the complexation with Co(III) ion. After complexation, angular deformation was observed in the metal complex in the ligand fraction. Due to this deformation, the lengths of the bonds C7N8, C10N11, C16N15 and C25 - N24 lengthen slightly. The bond lengths of the C=N groups that ranged from 1.276-1.285 Å in the free ligand elongate to 1.295-1.301 in the complex, while the bond lengths of C10-N11 (sp^3) group elongated from 1.464 to 1.476 Å [35]. However, the C18O23, C4-O12 and C31O33 bond length of 1.288, 1.291 and 1.265 Å are less than those of 1361, 1371 and 1341 Å in free ligand. A similar behaviour was noticed for other bond lengths in cobalt complex. Slight variation in bond length values resulted in deviation of bond angle from standard values around the metal center. Bond angles $\angle O_{23}Co_{35}O_{12}$, $\angle O_{23}Co_{35}N15$, $\angle O_{12}Co_{35}N_8$, $\angle O_{23}Co_{35}N_8$, $\angle O_{23}Co_{35}N_{11}$, $\angle O_{12}Co_{35}N_{11}$ were 100.6°, 92.6°, 88.0°, 107.5°, 143.4° 110.4°, respectively, in the Co(III) complex. The complexation does not affect the bond length and bond angle values of the benzene skeleton and other remotely residing groups.

Electronic spectra and their frontier molecular orbitals: The UV-visible spectra of H_3L and its Co(III) complex in ethanol are shown in Fig. 2. Prior to the complexation of the ligand, the absorption maxima were recorded at 345 nm, attributed to transition n→π* [30-34]. In case of the Co(III) complex, the maximum band with respect to the ligand band was shifted to 449 nm because of the extension of the larger conjugated system after coordination driving the interaction of the LMCT. In order to understand deeply, the simulated UV-visible spectra of H_3L and complex were calculated by TD-DFT/B3LYP/6-311G (d,p) in ethanol. GaussSum 2.2 was applied to calculate and prepare the contributions of groups to molecular orbitals and UV-visible spectra respectively. It can be seen that the UV-visible spectra obtained with TD-DFT B3LYP 6-311G (d,p) [29,35] are theoretically calculated. Solvent effects generated larger absorption bands [36] and that the transition at 490 and 345 nm corresponds to β-spin HOMO-LUMO and α-spin HOMO-LUMO with 55 and 52 transition contribution, respectively. The other has two peaks at 327 and 326 nm are due to π→π* HOMO-LUMO with 70 and 74 % contribution in the electronic transition. In case of the ligand, the theoretical UV-visible spectrum was observed important transitions at 321 and 318 nm that correspond to the various HOMO-LUMO strata with a transition contribution of 93 and 89 % in the spectrum. Other bands observed at 254 and 251 with 94 and 93 % transition contributions appeared because of the origin π→π*.

The isodensity plots of Co(III) complex along with the energy values of HOMO and LUMO molecular orbitals are depicted in Fig. 3. The low HOMO and LUMO gap gives an idea of the biological chemical reactivity and low kinetic stability of the present complex. The dipole moment, SCF energy and HOMO-LUMO energy gap, indices are computed at TD-DFT/B3LYP 6-311G(d,p) level of theory shown in Table-1.

The molecular electrostatic potential (MEP) map of the Co(III) complex is calculated and used to study the binding properties are displayed in Fig. 4. The -ve MEP is found on the oxygen atoms, as indicated by a slight red colour [37,38] (Fig. 4). The +ve and -ve potential of MEP for the studied

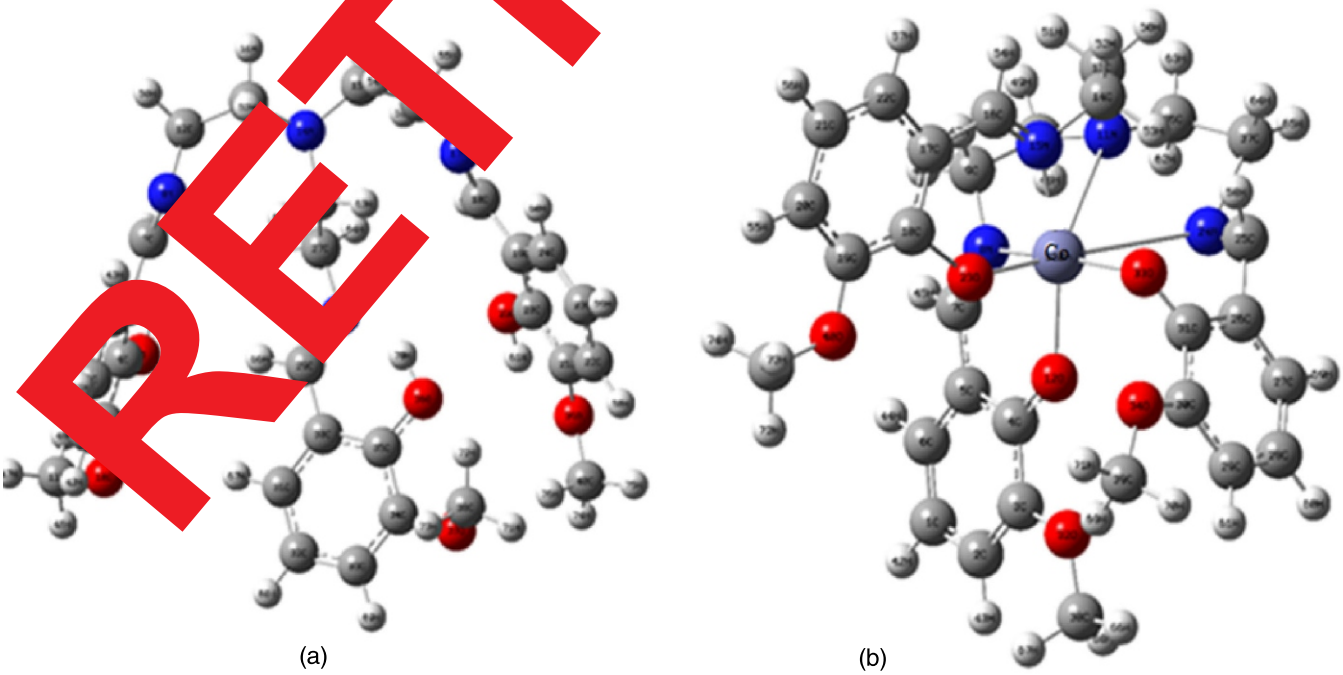

(a) (b)

Fig. 1. Optimized geometry of ligand and its Co(III) complex

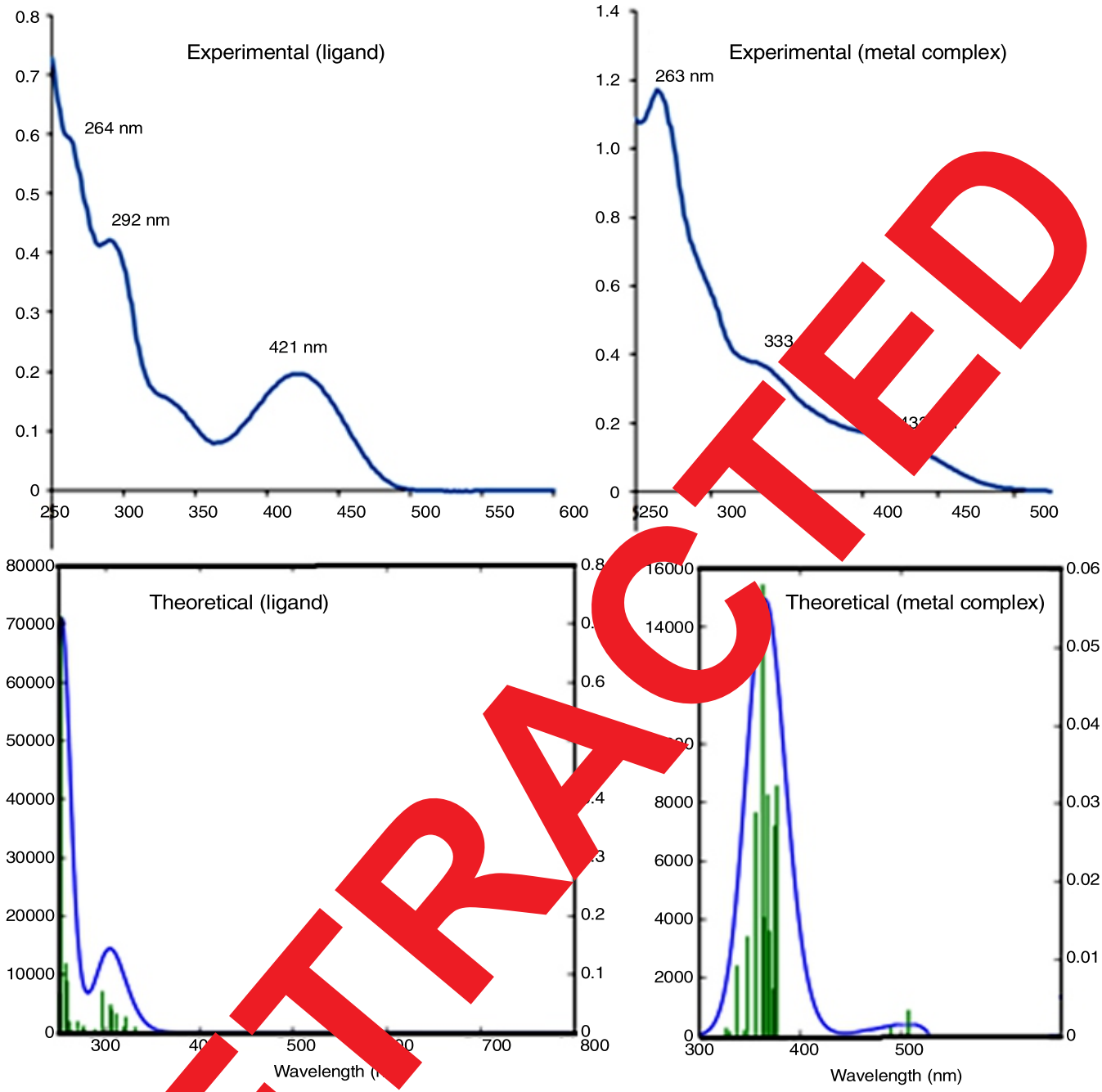

Fig. 2. Experimental and calculated UV-visible spectra of ligand and its Co(III) complex in ethanol

Co(III) complex is pr d site f ucleophilic and electrophilic at

Mulliken charge population and other properties: Mu ens char [37-39] can be used as a fast and qualitative gui th es in the molecules to obtain prior informa n properties associated with systems. The charge distributio ligand and its Co(III) complex calculated by the Mullik ethod were given by the corresponding Mullikens plots in Fig. 5. Molecular properties [40] such as thermodynamic parameters, dipole moment and descriptors of chemical reactivity are important and are based on HOMO-LUMO and its energy gap. Thermodynamic data such as thermal energy, molar heat capacity and entropy of the complex are given in Table-1.

Conclusion

The Co(III) complex was synthesized by the reaction of H_3L with cobalt(III) chloride in ethanol. The Co(III) complex was characterized by spectral and DFT calculations in order to know the bonding mode inside into the structure.

ACKNOWLEDGEMENTS

This work was funded by the Deanship of Scientific Research at Princess Nourah bint Abdulrahman University, through the Research Groups Program Grant no. (RGP-1438-00).

CONFLICT OF INTEREST

The authors declare that there is no conflict of interests regarding the publication of this article.

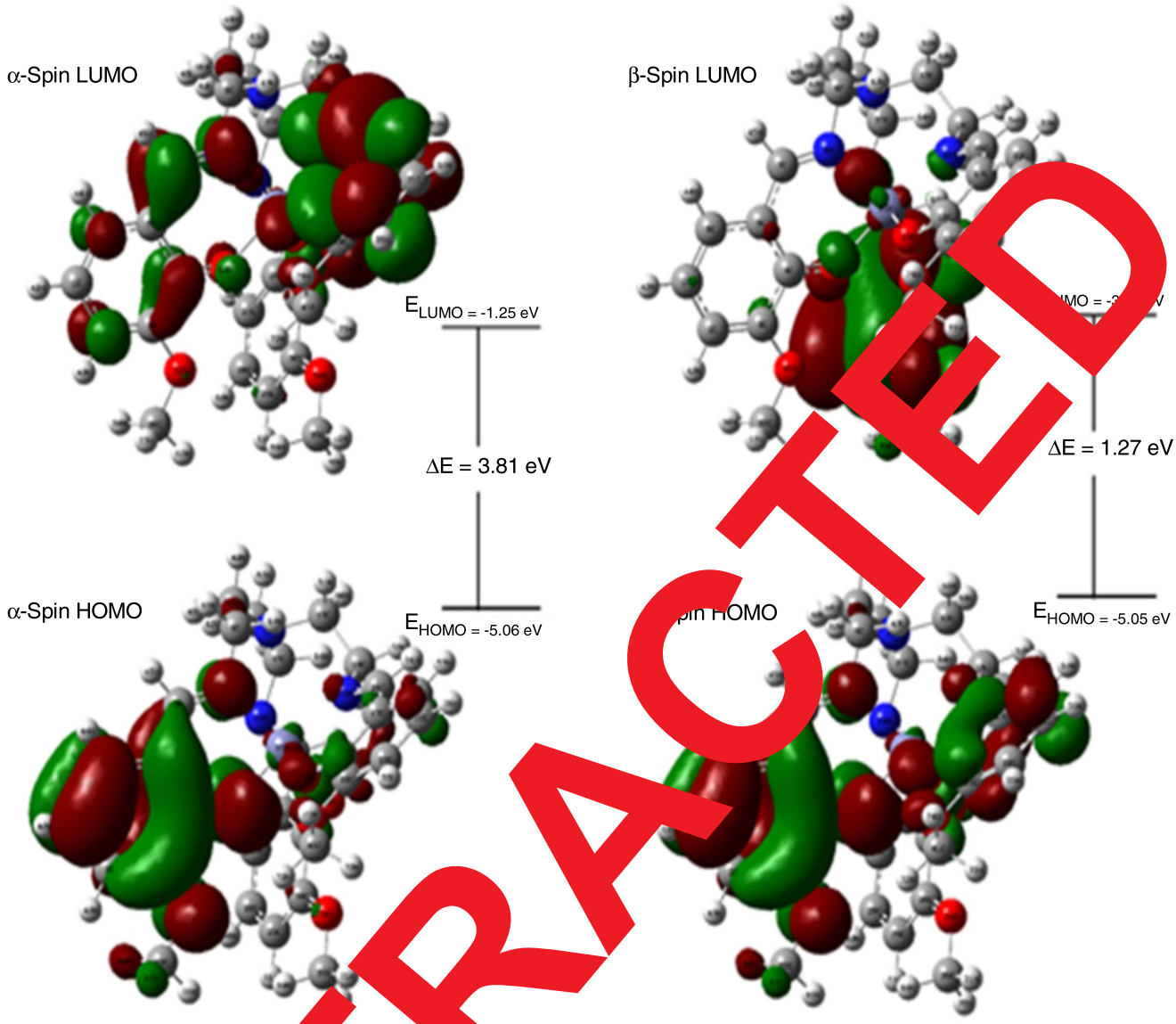

Fig. 3. ...O and LUMO of Co(III) complex

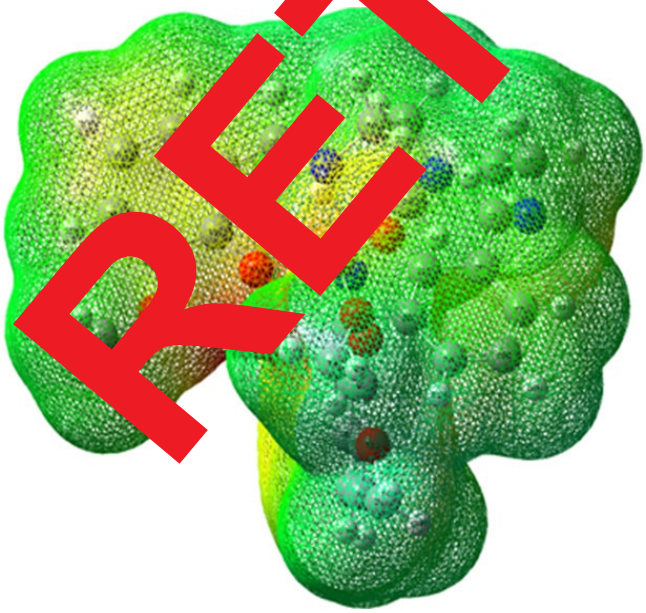

Fig. 4. MEP surface of Co(III) complex

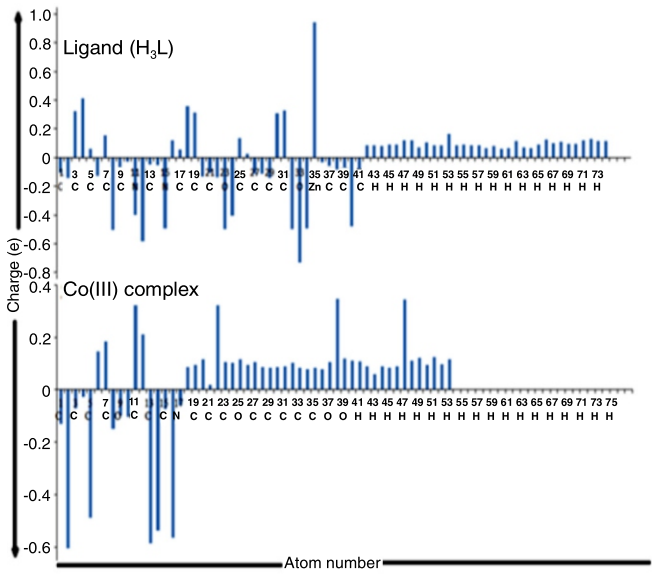

Fig. 5. Mulliken charge distribution of ligand and its Co(III) complex

TABLE-1
CALCULATED SCF ENERGY, ZERO-POINT VIBRATIONAL ENERGY, THERMODYNAMIC QUANTITIES (AT 298.15 K), DIPOLE MOMENT, ENERGIES OF FRONTIER MOLECULAR ORBITALS AND GLOBAL REACTIVITY DESCRIPTORS OF COMPLEX

Parameters	B3LYP with 6-311G(d, p)
SCF energy (kcal/mol)	-2266927.9
Zero point vibrational energy (kcal/mol)	373.25461
Total thermal energy (kcal/mol)	397.258
Molar heat capacity at const. volume, Cv (cal mol^{1} K^{1})	148.272
Total entropy, S (cal mol^{1} K^{1})	230.818
Field independent dipole moment (Debye)	
μx	-2.2018
μy	-0.2290
μz	-0.6124
μtotal	2.2968
Frontier MO energies (eV)	
LUMO (α-spin)	-1.25
LUMO (β-spin)	-3.78
HOMO (β-spin)	-5.05
HOMO (α-spin)	-5.06
GAP= LUMO-HOMO (α-spin), LUMO-HOMO (β-spin)	3.81 (α-spin), 1.27 (β-spin)
Global reactivity descriptors (eV)	
Hardness	1.905
Chemical potential	-3.15
Electrophilicity index	2.60
Electronegativity	3.15
Ionization potential	5.05
Softness	0.524

REFERENCES

1. M. Asadi, S. Torabi and K. Mohammadi, *Sp… him. A… A Mol. Biomol. Spectrosc.*, **122**, 676 (2014); https://doi.org/10.1016/j.saa.2013.09.098.
2. D. Sinha, A.K. Tiwari, S. Singh, G. Shukla, P… handra a… A.K. Mishra, *Eur. J. Med. Chem.*, **43**, … (200… https://doi.org/10.1016/j.ejmech.20…5.022.
3. R. Ramesh and S. Maheswaran, … *rg. Biochem.*, **9**… 2003); https://doi.org/10.1016/S0162…00237-X.
4. M.K. Biyala, K. Sharma, M. S…, …i and R.V. Singh, *Transition Met. Chem.*, **33**, 377 (2008); https://doi.org/10.1007/…1243-008-9053-…
5. S. Bawa and S. Kum… *ian J. Chem.*, **48B**, … 009).
6. A. Jarrahpour, D. Kh… E. De Clercq, C. Salmi and … Brunel, *Molecules*, **12**, 1720 (2007); https://doi.org/…90/120…0.
7. D.J. Berg, S.J… and C… ig, *J. Am… hem. Soc.*, **113**, 2528 (1991); https://doi.org/1…007a029.
8. R.M. Kirchner, C. M… J. Bailey, … Howe, L.P. Torre, L.J. Wilson, L.C. A… N.J. Ro… F.C… gafelter, *Coord. Chem. Rev.*, **77**, 89 (…); h… doi.or… .1016/0010…5(87)85033-6.
9. … Ragun… n and P.K. Bharadwaj, *J. Chem. Soc., Dalton Trans.*, … 7 (199…; …/d… …920002417.
10. M… N. Kocak, U. Sayin and M. Yilmaz, *J. Macromol. Sci. Part A Pure …hem.*, **49**, 603 (2012); https://d… …0.1080/10601325.2012.696988.
11. J.-P. Costes, … upuis, G. Commenges, S. Lagrave and J.-P. Laurent, *Inorg. Chim. Acta*, **285**, 49 (1999); https://doi.org/10.1016/S0020-1693(98)00303-X.
12. J.-P. Costes, F. Dahan, A. Dupuis, S. Lagrave and J.-P. Laurent, *Inorg. Chem.*, **37**, 153 (1998); https://doi.org/10.1021/ic9712481.
13. E.C. Alyea, S. Liu, B. Li, Z. Xu and X. You, *Acta Crystallogr.*, **C45**, 1566 (1989); https://doi.org/10.1107/S0108270189002283.
14. C.J. Frederickson, *Int. Rev. Neurobiol.*, **31**, 145 (1989); https://doi.org/10.1016/S0074-7742(08)60279-2.
15. G. Danscher, G. Howell, J. Perez-Clausell and N. Hertel, *Histochemistry*, **83**, 419 (1985); https://doi.org/10.1007/BF00509203.
16. J. Perez-Clausell and G. Danscher, *Brain Res.*, **337**, 91 (1985); https://doi.org/10.1016/0006-8993(85)91612-9.
17. L. Slomianka, G. Danscher and C.J. Frederickson, *Neuroscience*, **38**, 843 (1990); https://doi.org/10.1016/0306-4522(90)90076…
18. B.A. Masters, C.J. Quaife, J.C. Erickson, E… …ly, G.J. F… B.P. Zambrowicz, R.L. Brinster and R.D. Palmite… *…eurosci.*, **14**, 584… …94); https://doi.org/10.1523/JNEUROSCI.1…5844.1994.
19. P.Q. Trombley, M.S. Horning, L. J. Blakemo… *…hemistry (Mo… …v)*, **65**, 807 (2000).
20. M.J. Frisch, G.W. Trucks, H.B… …egel, G.E. S… …M… …Robb, J.R. Cheeseman, G. Scalmani… …arone, G.A. Peters… …ukatsuji, X. Li, M. Caricato, A.V. Mar… …J. Bloi… G. Janesko… Gomperts, B. Mennucci, H.P. Hratchi… V. Ortiz… …zmaylov, J.L. Sonnenberg, D. Williams-Young, F. Di… …ipp…, F. Egidi… …oings, B. Peng, A. Petrone, T. Hende… …n, D… …ne, V.G. Z… …ewski, J. Gao, N. Rega, G. Zheng, W… …ng, M. H… …Ehar… Toyota, R. Fukuda, J. Hasegawa, M… …da, T. Nakajim… …O. Kitao, H. Nakai, T. Vreven, K. T… …J.A. Montgome… …E. Peralta, F. Ogliaro, M.J. Bearp… …E.N. Brothers, K… …N. Kudin, V.N. Staroverov, T.A. Keit… Koba… …Normand, K. Raghavachari, A.P. Rendell, J.C. Burant, S.S. Iyenga… …masi, M. Cossi, J.M. Millam, M. Klene, C. Adamo, R. Cammi, J.W… …rski, R.L. Martin, K. Morokuma, O. F… Foresman and D… …x, Gaussian, Inc., Wallingford CT, …).
21. … Delley, *J. Chem. Phys.*, **92**, 508 (1990); …tps://doi.org/10…3/1.458452.
22. … Delley, *J. Che… …ys.*, **113**, 7756 (2000); …s://doi.org/10… …3/1.1316015.
23. … …s Softwar… …, Material Studio Modeling Environment, Accelrys So… …Diego, Release v7.0 (2013).
24. M.S. N… …S. Joseyphus, *Spectrochim. Acta A Mol. Biomol. Spectrosc.*, **70**, 749 (2008); …//doi.org/10.1016/j.saa.2007.09.006.
25. … …aghi, S. Moradi, S. Salehzadeh and A.G. Blackman, *J. Mol. Struct.*, **1108**, 727 (2016); https://doi.org/10.1016/j.molstruc.2015.12.052.
26. S. Salehzadeh, S.M. Nouri, H. Keypour and M. Bagherzadeh, *Polyhedron*, **24**, 1478 (2005); https://doi.org/10.1016/j.poly.2005.03.099.
27. N. Deligonul, M. Tumer and S. Serin, *Transition Met. Chem.*, **31**, 920 (2006); https://doi.org/10.1007/s11243-006-0087-0.
28. K. Nakamoto, Infrared Spectra of Inorganic and Coordination Compounds, Wiley, Interscience: New York (1970).
29. S.A. Abdel-Latif, H.B. Hassib and Y.M. Issa, *Spectrochim. Acta A Mol. Biomol. Spectrosc.*, **67**, 950 (2007); https://doi.org/10.1016/j.saa.2006.09.013.
30. S. Zolezzi, A. Decinti and E. Spodine, *Polyhedron*, **18**, 897 (1999); https://doi.org/10.1016/S0277-5387(98)00376-3.
31. Y.L. Zhang, W.J. Ruan, X.J. Zhao, H.G. Wang and Z.A. Zhu, *Polyhedron*, **22**, 1535 (2003); https://doi.org/10.1016/S0277-5387(03)00261-4.
32. F. Gao, W.J. Ruan, J.M. Chen, Y.H. Zhang and Z.A. Zhu, *Spectrochim. Acta A Mol. Biomol. Spectrosc.*, **62**, 886 (2005); https://doi.org/10.1016/j.saa.2005.03.021.
33. E. Runge and E.K.U. Gross, *Phys. Rev. Lett.*, **52**, 997 (1984); https://doi.org/10.1103/PhysRevLett.52.997.
34. R. Bauernschmitt and R. Ahlrichs, *Chem. Phys. Lett.*, **256**, 454 (1996); https://doi.org/10.1016/0009-2614(96)00440-X.
35. Y. Li, Z. Yang, B. Song, H. Xia and Z. Wang, *Inorg. Nano-Met. Chem.*, **47**, 966 (2017); https://doi.org/10.1080/24701556.2016.1278554.
36. I. Rajaei and S.N. Mirsattari, *J. Mol. Struct.*, **1163**, 236 (2018); https://doi.org/10.1016/j.molstruc.2018.02.010.
37. S. Muthu, T. Rajamani, M. Karabacak and A.M. Asiri, *Spectrochim. Acta Acta A Mol. Biomol. Spectrosc.*, **122**, 1 (2014); https://doi.org/10.1016/j.saa.2013.10.115.
38. P. Politzer and J.S. Murray, *Theor. Chem. Acc.*, **108**, 134 (2002); https://doi.org/10.1007/s00214-002-0363-9.
39. C.J. Dhanaraj and J. Johnson, *J. Coord. Chem.*, **68**, 2449 (2015); https://doi.org/10.1080/00958972.2015.1051475.
40. S.A.A. Nami, N. Sarikavakli, M.J. Alam, M. Alam, S. Park and S. Ahmad, *J. Mol. Struct.*, **1138**, 90 (2017); https://doi.org/10.1016/j.molstruc.2017.03.004.